Pakistan Veterinary Journal
ISSN: 0253-8318 (PRINT), 2074-7764 (ONLINE)
DOI: 10.29261/pakvetj/2025.284

RESEARCH ARTICLE

Reutilization of SKQ1's antibacterial and anti-quorum sensing activities to combat *Streptococcus suis* infection

Shuo Yuan[1,2,3†], Zhaoyu Yi[1†], Jingyi Wu[1], Shuji Gao[1], Yingying Quan[1], Wenjie Jin[1], Baobao Liu[1], Yuxin Wang[1], Shaohui Wang[3]*, Li Yi[2]* and Yang Wang[1]*

[1]College of Animal Science and Technology, Henan University of Science and Technology, Luoyang 471000, China; [2]College of Life Science, Luoyang Normal University, Luoyang 471934, China; [3]Shanghai Veterinary Research Institute, Chinese Academy of Agricultural Sciences, Shanghai, China
† These authors contributed equally to this work.
*Corresponding author: wangyocean@163.com; lilili123168@163.com; shwang@shvri.ac.cn

ARTICLE HISTORY (25-707)

Received:	July 27, 2025
Revised:	October 02, 2025
Accepted:	October 04, 2025
Published online:	October 21, 2025

Key words:
AI-2 QS
Biofilm
SKQ1
Streptococcus suis
Virulence

ABSTRACT

Streptococcus suis (*S. suis*) is a significant zoonotic pathogen. Owing to the widespread use of antibiotics in agriculture and farming, multidrug-resistant *S. suis* is proliferating, posing severe public health concern. The AI-2 quorum sensing (QS) system is a ubiquitous intercellular communication mechanism in both Gram-positive and Gram-negative bacteria, including *S. suis*, enabling it to coordinate fundamental life processes, adapt to environmental changes, develop antibiotic tolerance, and enhance virulence. In this study, SKQ1 demonstrated potent bacteriostatic and bactericidal activity against *S. suis*, with a lower propensity for resistance development. Mechanistic analyses indicate that this effect is likely achieved by compromising the integrity and functionality of the cytoplasmic membrane. Additionally, sub-inhibitory concentrations of SKQ1 significantly inhibited biofilm formation and reduced the virulence of *S. suis*. Untargeted metabolomics revealed that this effect may be mediated through disruption of the AI-2 QS system associated with methionine metabolism. Further investigations demonstrated that SKQ1 reduced the production of AI-2 signaling molecules, thereby diminishing biofilm formation and virulence. Owing to its antimicrobial activity and interference with the AI-2 QS system, SKQ1 exhibited robust therapeutic efficacy against diverse models of *S. suis* infection, including human isolates, multidrug-resistant strains, and highly virulent strains. This study offers novel insights into antibiotic strategies for managing porcine streptococcal infections and addressing the drug resistance crisis in *S. suis*.

To Cite This Article: Yuan S, Yi Z, Wu J, Gao S, Quan Y, Jin W, Liu B, Wang Y, Wang S, Yi L and Wang Y, 2025. Reutilization of SKQ1's antibacterial and anti-quorum sensing activities to combat *Streptococcus suis* infection. Pak Vet J. http://dx.doi.org/10.29261/pakvetj/2025.284

INTRODUCTION

Streptococcus suis (*S. suis*) is a significant zoonotic pathogen capable of causing meningitis, pneumonia, and arthritis in both humans and pigs, which can result in fatal outcomes in severe cases (Lun *et al.*, 2007). *S. suis* is prevalent in pig farms, with epidemiological studies indicating that up to 95% of pigs may carry the pathogen, leading to substantial economic losses in the pig industry (Obradovic *et al.*, 2021; Werinder *et al.*, 2020). Moreover, *S. suis* can be transmitted to humans via the slaughter of live pigs or consumption of undercooked pork, posing significant risks to public health and societal stability (Lun *et al.*, 2007). The first documented human cases of *S. suis* infection occurred in Denmark in 1968, followed by significant public health outbreaks in China in 1998 and 2005, resulting in hundreds of fatalities (Gao *et al.*, 2024a; Lun *et al.*, 2007).

Antibiotic resistance (AMR), particularly bacterial AMR, has become a critical global health challenge, jeopardizing the effectiveness of infection treatment and prevention. The use of antibiotics in animal agriculture for both prophylactic and therapeutic purposes is widespread and has exceeded that in human medicine. In 2017, it was estimated that approximately 73% of the total global consumption of antimicrobials was attributed to animal production (Van Boeckel *et al.*, 2015). The frequent and improper use of antibiotics in pig production has accelerated resistance development in *S. suis*, particularly against tetracyclines, macrolides, and lincosamides. This phenomenon may be attributed to the broad-spectrum activity of tetracyclines and the widespread use of the macrolide antibiotic tylosin as a growth promoter in pig farming (Uruén *et al.*, 2022). Alarmingly, the multidrug resistance rate of *S. suis* has shown a significant upward trend from 6% in 1999 to 23% in 2006, and multidrug resistant *S. suis* has now been isolated from human patients (Hoa *et al.*, 2011).

The swift rise of antimicrobial resistance in *S suis* highlights the pressing need for alternative therapeutic approaches. Despite this urgency, the discovery and development of new antibiotics remain highly challenging. As a result, repurposing existing non-antibiotic compounds—either used alone or in conjunction with traditional antimicrobials—may represent a promising strategy for controlling *S. suis* infections. For example, diacerein, a drug commonly used to treat degenerative joint diseases, has been shown to exert antibacterial activity and inhibit biofilm formation in various Gram-positive bacteria, including methicillin-resistant *S. aureus* (MRSA) (Sun *et al.*, 2025). Similarly, 5-fluorouracil, an anticancer drug, has demonstrated antimicrobial potential against *E. coli*, *S. aureus*, and *S. suis* (Sedlmayer *et al.*, 2021; Zhang *et al.*, 2024; Zuo *et al.*, 2024), and can act as a quorum-sensing quencher to suppress biofilm formation in pathogenic bacteria (Sedlmayer *et al.*, 2021).

QS refers to the intercellular communication process that occurs both within and between bacterial species. Bacteria utilize QS to coordinate essential life processes, enabling adaptation to their environment, resistance to threats, and competition with other species (Fan *et al.*, 2022). Bacteria detect the composition and density of microorganisms in complex environments through the production and detection of signaling molecules, thereby dynamically regulating their behavior (Abisado *et al.*, 2018; Fan *et al.*, 2022). The AI-2 QS system serves as the primary communication mechanism in *S. suis* and is a widely distributed communication system across diverse microorganisms. Given the extensive role of QS systems in regulating bacterial life activities, QS inhibitors are regarded as a promising antimicrobial strategy (Sedlmayer *et al.*, 2021).

SKQ1 (visomitin) is a plastoquinone derivative featuring a hydrophobic C10 linker attached to a triphenylphosphonium (TPP) cation. SKQ1 is primarily employed as a mitochondria-targeted antioxidant to treat ocular diseases linked to mitochondrial dysfunction, including dry eye and retinal disorders (Novikova *et al.*, 2014; Wei *et al.*, 2019), and its antimicrobial effect has only been sporadically reported (Dong *et al.*, 2023; Nazarov *et al.*, 2023a; Wu *et al.*, 2024).

This study demonstrated that SKQ1 exhibits potent antibacterial activity against *S. suis*, primarily by disrupting the cytoplasmic membrane, which ultimately results in bacterial rupture and cell death. Additionally, sub-inhibitory concentrations of SKQ1 interfere with the AI-2 QS system by disrupting methionine metabolism, thereby inhibiting *S. suis* biofilm formation and reducing its virulence. Leveraging its antimicrobial and QS inhibition effects, SKQ1 demonstrated therapeutic efficacy in a *Galleria mellonella* infection model of *S. suis*, including multidrug-resistant strains. In summary, SKQ1 represents a promising drug candidate for the treatment of *S. suis* infections.

MATERIALS AND METHODS

Bacterial strains and cell lines: This study utilized *S. suis* serotype 2 strains, including HA9801 and *ZY05719* (human-derived isolates), *P1/7* (a highly virulent strain), and *SLYFP25* (a multidrug-resistant clinical isolate). The Δ*LuxS* strain, a *LuxS* gene deletion mutant based on HA9801, was constructed in our previous work. Unless otherwise specified, 50 µL of overnight *S. suis* culture was inoculated into 5 mL of fresh TSB medium in a 12 mL culture tube and incubated in a shaking incubator at 37 °C and 180 rpm.

For experiments involving the *Galleria mellonella* infection model, S. suis was grown in TSB supplemented with 10% (v/v) fetal bovine serum (FBS) under identical culture conditions.

The mammalian cell lines PK-15, RAW264.7, Hep-2, and Marc-145 were maintained in DMEM medium (Gibco, USA) supplemented with 10% FBS (Vazyme Biotech Corp, Nanjing, China) at 37°C in a 5% CO_2 incubator.

SKQ1 was obtained from Aladdin, while the AI-2 precursor, DPD, was sourced from Omm Scientific, Inc. Unless otherwise indicated, AI-2 was used at a final concentration of 4 µM in all experiments.

Determination of MIC and MBC: The MIC and MBC were determined using the broth microdilution method based on the guidelines of the Clinical and Laboratory Standards Institute (CLSI) (Koeth, DiFranco-Fisher, and McCurdy, 2015).

Resistance Induction: Resistance induction experiments were conducted for SKQ1 and four antibiotics (tylosin, ampicillin, ciprofloxacin, and gentamicin) under identical conditions. Overnight cultures of *S. suis* were inoculated into TSB medium containing each drug at a concentration of 1/2 MIC. After 24 hours of incubation, the bacterial culture was passaged into fresh TSB medium supplemented with the same antibiotic, marking the end of the first generation of induction. This process was repeated for 25 generations, with MIC values reassessed every five generations.

Time-Kill curves: The *S suis* cultures were grown under the aforementioned conditions for 8 hours until the late exponential growth phase. The bacterial cultures were diluted 1:100 into fresh 5 mL TSB medium and exposed to SKQ1 at final concentrations of 1.25, 2.5, 5, and 10 µg/mL. As a control, 0.1% DMSO was used. Incubation was carried out at 37 °C with agitation at 180 rpm. At 0, 2, 4, 6, and 8 hours, 200 µL aliquots were withdrawn for count.

The collected samples were centrifuged (6000 rpm, 5 minutes, 4°C), washed with sterile PBS to remove residual drugs, serially diluted, and plated on TSA agar. Following 24 hours of incubation at 37°C, CFUs were counted to determine viable bacterial numbers. All experiments were conducted in triplicate.

Persister cells eradicating assay: Based on previous studies, the proportion of persister cells in bacterial populations increases significantly during the stationary phase (Conlon *et al.*, 2016; Willenborg *et al.*, 2014). Persister cells were enriched using an established method (Tang *et al.*, 2024) Briefly, *S. suis* were inoculated into TSB medium at a 1:100 ratio and grown for 24 hours to reach the late stationary phase. To eliminate non-persister cells, the cultures were exposed to ciprofloxacin at a final concentration of 60 µg/mL for a duration of 6 hours. The cultures were then centrifuged to remove residual ciprofloxacin, and the bactericidal effect of SKQ1 on persister cells was assessed using the method described in the Time-Kill curves assay.

Assessment of antiphagocytic ability: The effect of SKQ1 on the anti-phagocytic ability of *S. suis* was evaluated according to previously reported methods (Yuan *et al.*, 2025).

Intracellular killing assay: The intracellular killing assay was performed similarly to the antiphagocytic ability test, with the following modifications: after killing extracellular *S. suis* with 0.1 mg/mL vancomycin and 5 µL of lysozyme, the cells were washed with sterile PBS and incubated in DMEM medium containing SKQ1 (5 µg/mL), ciprofloxacin (100 µg/mL), or ampicillin (100 µg/mL) for 3 hours at 37℃.

Following drug treatment, the cells were washed with PBS to remove residual drugs, lysed using an ice-water mixture, and the lysates were serially diluted and plated on TSA agar. CFUs were counted after 24 hours of incubation at 37℃.

DNA leakage: DNA leakage was assessed with minor modifications based on a previously reported protocol (Tang *et al.*, 2024). *S suis* were diluted 1:100 in TSB and incubated for 8 hours. The resulting bacterial suspension was centrifuged at 8000 rpm for 5 minutes, and the pellet was washed with sterile PBS. After washing, the pellet was resuspended in PBS and exposed to SKQ1 at concentrations corresponding to 2×, 4×, and 8× the MIC.

At predetermined intervals (0, 2, 4, 6, and 8 hours), 500 µL aliquots were collected, passed through 0.22 µM filters to remove bacterial cells, and the DNA released into the filtrate was quantified by measuring absorbance at 260 nm using a micro-spectrophotometer.

Assessment of cell membrane permeability: Cell membrane permeability was evaluated following an established method (Li *et al.*, 2024). Eight-hour cultures of S. suis were centrifuged and resuspended in 0.01 mol/L PBS to adjust the bacterial suspension to an OD600 of approximately 0.5. Propidium iodide (PI) was added to the suspension at a final concentration of 10 nM, and the mixture was incubated in the dark at 37℃ for 20 minutes. SKQ1 was then added at concentrations of 2, 4, and 8×MIC. Following 6 hours of incubation, fluorescence intensity was recorded using an excitation wavelength of 535 nm and an emission wavelength of 615 nm.

Scanning electron microscopy (SEM) and transmission electron microscopy (TEM): To observe morphological changes in *S. suis* after SKQ1 treatment, overnight cultures were diluted 1:100 in TSB medium and grown for 8 hours to reach the late exponential growth phase. The bacterial suspension was incubated with SKQ1 at concentrations of 2×, 4×, and 8× MIC for 8 hours. After treatment, bacterial cells were harvested by centrifugation, rinsed with PBS, and fixed in 2.5% glutaraldehyde at 4 °C overnight. Subsequently, the samples were washed with deionized water and dehydrated through a graded ethanol series (10, 30, 50, 70, 90, and 100%), with each step lasting 10 minutes. The dehydrated specimens were air-dried at room temperature and examined using a SEM.

For biofilm analysis, glass coverslips were placed in 6-well plates containing TSB supplemented with SKQ1 at 1/2, 1/4, and 1/8×MIC. *S. suis* was inoculated at a 1:100 ratio and incubated statically at 37℃ for 36 hours. Subsequent sample preparation for biofilm imaging followed the same steps as described for SEM observations.

To investigate intracellular alterations, overnight *S. suis* cultures were diluted 1:100 into TSB supplemented with SKQ1 at 1/2, 1/4, and 1/8× MIC and incubated for 16 hours. Bacterial cells were then harvested and fixed in 2.5% glutaraldehyde at 4 °C overnight. The samples were subsequently treated with 2% osmium tetroxide for 2 hours, dehydrated using a graded ethanol series, embedded in epoxy resin, and examined by TEM (H-7650; Hitachi, Tokyo, Japan).

***Galleria mellonella* infection model:** *S. suis* were grown in TSB containing 10% (v/v) fetal bovine serum for 12 hours, centrifuged, and resuspended in PBS to approximately 1×10^7 CFU/mL. 10 µL sample was injected into the larvae between the second-to-last pair of legs. The PBS group was injected with sterile PBS instead of the bacterial suspension.

Thirty minutes post-injection, larvae were treated with SKQ1 at 1.25, 2.5, and 5 mg/kg, using the same injection method. The control group received 0.1% DMSO, and the PBS group was re-injected with PBS to assess the impact of the injection procedure on the larvae. The larvae were then monitored for 72 hours, with survival being recorded every 6 hours. Death was defined as the absence of life activity after gentle prodding. Photographs were taken 36 hours post-injection to avoid decomposition of deceased larvae, and all carcasses were disposed of responsibly.

To assess SKQ1's impact on *S. suis* virulence, bacteria were cultured in TSB containing 10% (v/v) fetal bovine serum and SKQ1 at 1/2, 1/4, and 1/8×MIC for 12 hours. After centrifugation and resuspension in PBS (final concentration ~1×10^7 CFU/mL), the larvae were injected as described, and survival was recorded over 72 hours.

Extracellular polysaccharide (EPS) content: Overnight S. suis cultures were inoculated into TSB medium and grown for 24 hours. The supernatant was collected by centrifugation (6000 rpm, 10 min)(Gao *et al.*, 2024b). Ethanol (three volumes) was added to the supernatant and incubated at 4°C for 12 hours to precipitate EPS. The precipitate was collected by centrifugation, resuspended in 1 mL ultrapure water, and mixed with phenol (6%) and concentrated sulfuric acid in a ratio of 2:1:5. The mixture was incubated in a water bath at 60°C for 20 minutes. The OD490 was measured, and EPS content was determined using a standard curve equation (Li *et al.*, 2022).

Capsular Polysaccharide (CPS) Content: *S. suis* was cultured in TSB medium supplemented with SKQ1 at 1/2, 1/4, and 1/8× MIC. CPS was extracted according to previously described methods (Yuan *et al.*, 2025). CPS levels were quantified using the sulfuric acid–phenol assay, with absorbance measured at 490 nm. The CPS concentration was determined based on a previously established standard curve (Gao *et al.*, 2024a).

Biofilm quantification: Biofilm formation was assessed as previously described (Gao *et al.*, 2025).

Viable bacterial count in biofilm: Biofilm cultivation was conducted as described above. After removing the supernatant, the biofilm was washed with PBS to eliminate planktonic bacteria. TSB medium containing SKQ1 at concentrations of 2, 4, and 8×MIC was added to each well; the control group contained 0.1% DMSO. Each well received 200 µL of the respective solution. After incubation at 37°C for 6 hours, the supernatant was discarded, and the biofilm was resuspended and thoroughly mixed. The suspension was serially diluted, plated on TSA agar, and incubated for CFU counting.

Untargeted metabolomics: *S. suis* were transferred into fresh TSB or TSB supplemented with SKQ1 at 1/8× MIC. Following 10 hours of incubation, the optical density at 600 nm was adjusted to 0.6. The bacterial cultures were then centrifuged, and the supernatant was discarded. The resulting pellet was rapidly quenched with liquid nitrogen and resuspended in 1 mL of pre-chilled extraction solution (methanol:acetonitrile:water = 2:2:1, v/v/v). Cell lysis was performed via sonication, followed by centrifugation, and the supernatant was filtered through a 0.22 µM membrane for subsequent analysis.

The LC–MS/MS conditions were based on previous studies (Gao *et al.*, 2024a). Data were processed and visualized using MetaboAnalyst 6.0 (Pang *et al.*, 2024).

Growth curve: Overnight *S. suis* cultures were transferred to TSB medium containing SKQ1 at concentrations of 1/2, 1/4, and 1/8×MIC. Cultures grow under the above conditions. Samples (2 mL) were collected at designated time points (0, 2, 4, 6, 8, 10, and 12 hours), and OD600 was measured using a spectrophotometer. Three independent biological replicates were performed.

AI-2 signal molecule quantification: AI-2 quantification was conducted following an established method (Han and Lu, 2009). Overnight *S. suis* cultures were transferred to TSB medium with or without SKQ1 (1/8×MIC) and and grow normally for 10 hours. At designated time points, 1 mL samples were collected, centrifuged (10,000 rpm, 4°C, 10 minutes), and filtered through a 0.22 µM filter. The negative control was prepared using supernatants collected from *E. coli DH5α* cultures grown under identical conditions (Surette and Bassler, 1998).

The *Vibrio harveyi* BB170 reporter strain was cultured for 16 hours at 30°C with aeration (175 rpm), then diluted 1:5000 in fresh AB medium. A mixture of 90 µL of the diluted BB170 culture and 10 µL of AI-2 supernatant from the test group was incubated at 28°C in the dark for 6 hours. Bioluminescence was measured at 490 nm using a Promega Luminometer. The ratio of the experimental group's bioluminescence to the negative control was calculated to assess AI-2 activity.

Hemolytic activity assay: Fresh pig whole blood was centrifuged (2000 rpm, 10 minutes), and the supernatant was discarded. The red blood cells (RBCs) were washed three times with sterile PBS to obtain a 5% RBC suspension. Equal volumes of SKQ1 at different concentrations (as indicated in Fig. 7B) were added to the suspension. After incubation at 37 °C for 1 hour, the samples were centrifuged, and the supernatants were transferred into 96-well plates. Absorbance at 570 nm was then recorded.

Cytotoxicity detection by CCK-8: PK-15, RAW264.7, Hep-2, and Marc-145 cell lines were cultured overnight. After discarding the supernatants, DMEM containing SKQ1 (0.0625–8 µg/mL) and 2% serum was added to the cells. DMEM supplemented with 0.1% DMSO was used as the negative control. Following 24 hours of incubation at 37 °C, 10 µL of CCK-8 reagent was added to each well and further incubated in the dark for 1 hour. Absorbance was then measured at 450 nm using a microplate reader.

Chequerboard assay: A 96-well plate was prepared by adding 100 µL of TSB to each well. SKQ1 at serially decreasing concentrations was added along the rows, and antibiotics at serially decreasing concentrations were added along the columns, forming an 8×8 matrix. Then, 100 µL of *S. suis* suspension (10^7 CFU/mL) was added to each well. The plate was incubated overnight at 37°C, and the absorbance at 600 nm was measured using a microplate reader.

Cell viabilities detection by Calcein-AM/PI staining: RAW264.7 and Hep-2 cells were cultured overnight. After discarding the supernatants, DMEM containing SKQ1 (2, 4, 8×MIC) and 2% serum was added. Cells were incubated at 37°C with 5% CO_2 for 12 hours. Subsequently, the cells were stained with 2 µM Calcein-AM and 10 µM propidium iodide (PI) for 30 minutes in the dark. Fluorescence microscopy was used to observe cell viability, with excitation/emission wavelengths of 494/514 nm for Calcein-AM and 493/636 nm for PI (Kennedy *et al.*, 2019).

RESULTS

SKQ1 exhibits broad-spectrum efficacy against various types of *S. suis*: SKQ1 [(10-(4,5-dimethyl-3,6-dioxocyclohexa-1,4-dien-1-yl) decyl) triphenyl phosphonium bromide], whose structure is depicted in Fig. 1A, is widely used as a peroxide inhibitor. To investigate the antibacterial activity of SKQ1 against *S. suis*, we initially assessed its inhibitory effect on human isolates using drug-sensitive paper discs, which revealed dose-dependent growth inhibition of *S. suis* (Fig. 1B). Subsequently, we determined the MIC of SKQ1 for several *S. suis* strains. As illustrated in Fig. 1C, SKQ1 demonstrated strong inhibitory effects across a broad range of *S. suis* strains, including human isolates, multidrug-resistant strains, highly virulent strains, and non-virulent strains, with MIC values ranging from 1.25

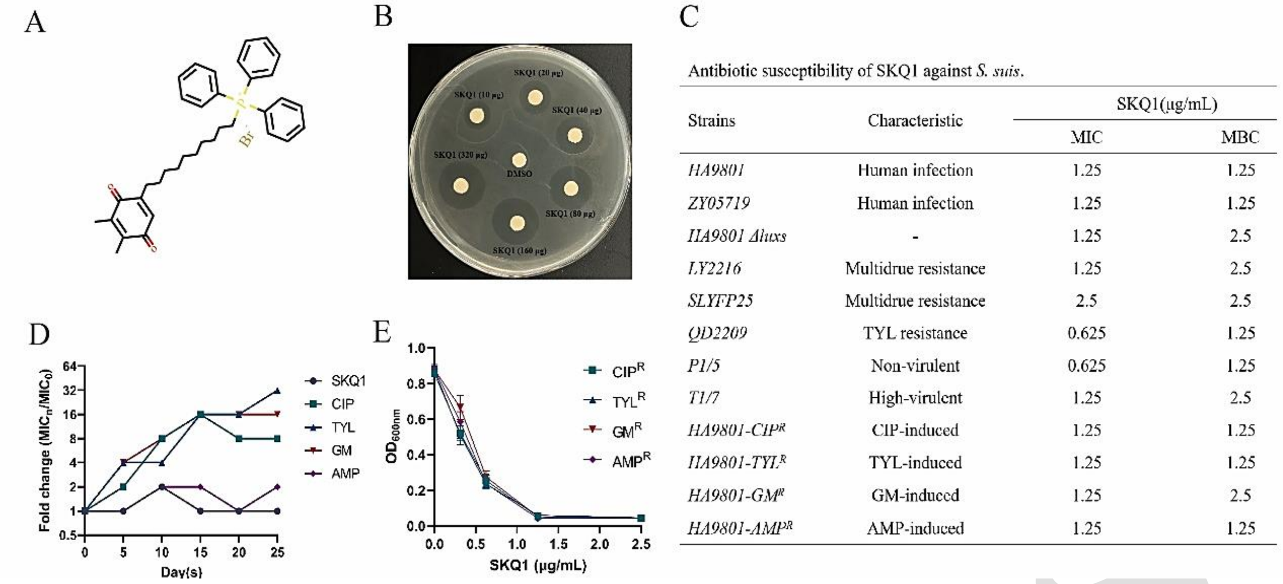

Antibiotic susceptibility of SKQ1 against *S. suis*.

Strains	Characteristic	SKQ1(μg/mL)	
		MIC	MBC
HA9801	Human infection	1.25	1.25
ZY05719	Human infection	1.25	1.25
HA9801 Δluxs	-	1.25	2.5
LY2216	Multidrue resistance	1.25	2.5
SLYFP25	Multidrue resistance	2.5	2.5
QD2209	TYL resistance	0.625	1.25
P1/5	Non-virulent	0.625	1.25
T1/7	High-virulent	1.25	2.5
HA9801-CIP^R	CIP-induced	1.25	1.25
HA9801-TYL^R	TYL-induced	1.25	1.25
HA9801-GM^R	GM-induced	1.25	2.5
HA9801-AMP^R	AMP-induced	1.25	1.25

Fig. 1: Inhibitory and bactericidal effects of SKQ1 against various *S. suis* strains. A: Chemical structure of SKQ1. B: Inhibitory activity of SKQ1 against *S. suis*, assessed using the drug-sensitive paper disc method. C: MIC and MBC of SKQ1 against different *S. suis* strains. D: Resistance development of *S. suis* under varying drug exposure conditions. E: Bacteriostatic efficacy of SKQ1 against laboratory-induced antibiotic-resistant *S. suis* strains.

to 2.5 µg/ml. We further broadened the scope of pharmacological sensitivity testing. The results, summarized in Table 1, confirmed that SKQ1 exhibited potent bacteriostatic and bactericidal activity against Gram-positive bacteria, such as *S. suis* and *Streptococcus agalactiae*, but showed limited activity against Gram-negative bacteria, including *Klebsiella pneumoniae* and *Escherichia coli*. These findings suggest that SKQ1 selectively targets Gram-positive bacteria. Considering that *S. suis* is frequently exposed to therapeutic agents in pig farms, assessing the rate of resistance development is crucial for evaluating SKQ1's potential as a therapeutic option. We therefore investigated resistance development by serially passaging *S. suis* with sub-inhibitory concentrations of SKQ1. Four clinically relevant antibiotics (aminoglycosides, fluoroquinolones, macrolides, and β-lactams) were included as controls for resistance induction, enabling us to compare resistance development in SKQ1 and evaluate potential cross-resistance. The results indicated no significant increase in *S. suis* resistance to SKQ1 over a 25-day resistance induction period. In contrast, MIC values for the other four antibiotics increased significantly, including an 8-fold increase for ciprofloxacin, a 32-fold increase for tylosin, a 16-fold increase for gentamicin, and a 2-fold increase for ampicillin (Fig. 1D). Notably, SKQ1 retained potent bacteriostatic activity against the antibiotic-resistant strains induced during the study (Fig. 1E). Collectively, these findings demonstrate that SKQ1 is effective against *S. suis* infections, exhibits broad-spectrum activity across diverse *S. suis* strains, and has no cross-resistance to clinically relevant antibiotics.

Bactericidal activity of SKQ1 against intracellular S. suis and persister cells: We evaluated the bactericidal activity of SKQ1 against S. suis using a time-kill curve assay. The results demonstrated that at 4× MIC, SKQ1 effectively reduced the bacterial population to below the detection limit within 8 hours, indicating robust bactericidal efficacy (Fig. 2A). Persister cells, a subpopulation of bacteria highly tolerant to antibiotics, can survive treatment, proliferate after antibiotic removal, and contribute to prolonged therapy and infection recurrence (Yuan et al., 2024). Persister cells predominantly arise during the stationary phase (Conlon et al., 2016), and in S. suis, increased tolerance to multiple antibiotics during the stationary phase compared to the exponential phase has been observed (Willenborg et al., 2014). Enrichment of S. suis persister cells was performed using established protocols (Tang et al., 2024). Subsequent bactericidal assays revealed that SKQ1 at 4× MIC reduced persister cell populations by approximately four orders of magnitude, reaching levels below the detection limit within 8 hours (Fig. 2B). Additionally, intracellular pathogens such as S. suis can evade antibiotics by exploiting host cells as protective niches (Liu et al., 2020b). Intracellular killing assays demonstrated that SKQ1 effectively eliminated intracellular S. suis, potentially due to its strong membrane permeability as a mitochondria-targeted antioxidant (Fig. 2C). In contrast, ampicillin and ciprofloxacin exhibited minimal activity against intracellular S. suis, consistent with findings from previous studies (Liu et al., 2020b) (Fig. 2C).

SKQ1 damages cell membranes to exert bactericidal effects: To investigate the mechanism underlying SKQ1's bactericidal effect on *S. suis*, we first observed the morphology of *S. suis* under varying concentrations of SKQ1 via scanning electron microscopy. The results clearly showed that SKQ1 caused dose-dependent damage to *S. suis*, characterized by indentations and perforations in the bacterial cell surface. Following treatment with 8×MIC SKQ1, *S. suis* cells lost their ellipsoidal morphology and became flattened (Fig. 2D). These observations suggested that SKQ1 induced cell membrane damage. To validate this hypothesis, we assessed cell membrane integrity using propidium iodide (PI), a dye that fluoresces red upon binding to DNA but is excluded by intact cell membranes. The fluorescence intensity indicated that SKQ1 caused dose-dependent membrane damage in *S. suis* (Fig. 2E).

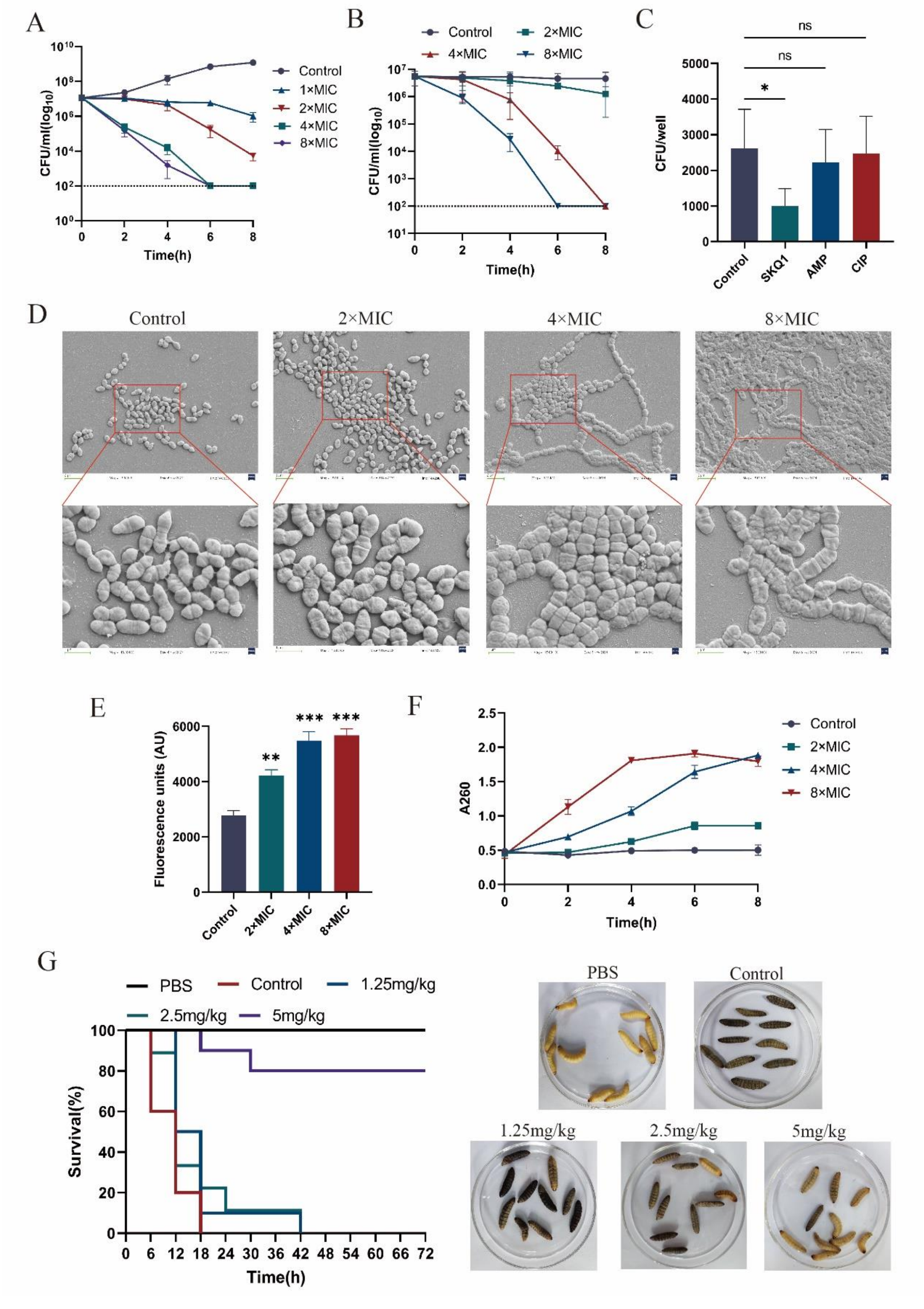

Fig. 2: Bactericidal effect of SKQ1 on *S. suis*. A: Time-kill curves of *S. suis* of SKQ1. B: Time-kill curves of *S. suis* persisters of SKQ1. C: Bactericidal effect of SKQ1 on intracellular *S. suis*. D: Scanning electron micrographs of *S. suis* treated with SKQ1. E: Cell membrane permeability of *S. suis* upon treatment with SKQ1. F: DNA leakage assay of *S. suis* subjected to varying concentrations of SKQ1. G: Therapeutic efficacy of SKQ1 in *S. suis*-infected *Galleria mellonella* larvae.

Further confirmation was provided by measuring DNA leakage from *S. suis* cells, which demonstrated time- and dose-dependent DNA release after SKQ1 treatment (Fig. 2). Collectively, these findings indicated a strong association between SKQ1's bactericidal mechanism and cell membrane rupture in *S. suis*, consistent with reports of SKQ1's effects on *S. aureus* (Wu *et al.*, 2024).

We then evaluated the therapeutic efficacy of SKQ1 against *S. suis* infection in *Galleria mellonella* larvae. Control *Galleria mellonella* larvae exposed to 0.1% DMSO succumbed within 18 h. Treatment with 1.25 mg/kg and 2.5 mg/kg SKQ1 slightly delayed larval death but did not reduce mortality at 72 h. However, treatment with 5 mg/kg SKQ1 increased larval survival by 80% and visibly reduced melanization (Fig. 2G). Additionally, we validated SKQ1's efficacy against other *S. suis* strains, including *ZY05719* (human isolate), *SLYFP25* (multi-resistant strain), and *P1/7* (highly virulent strain), using the *Galleria mellonella* model. As expected, SKQ1 exhibited robust therapeutic efficacy across all infection models (Fig. S1).

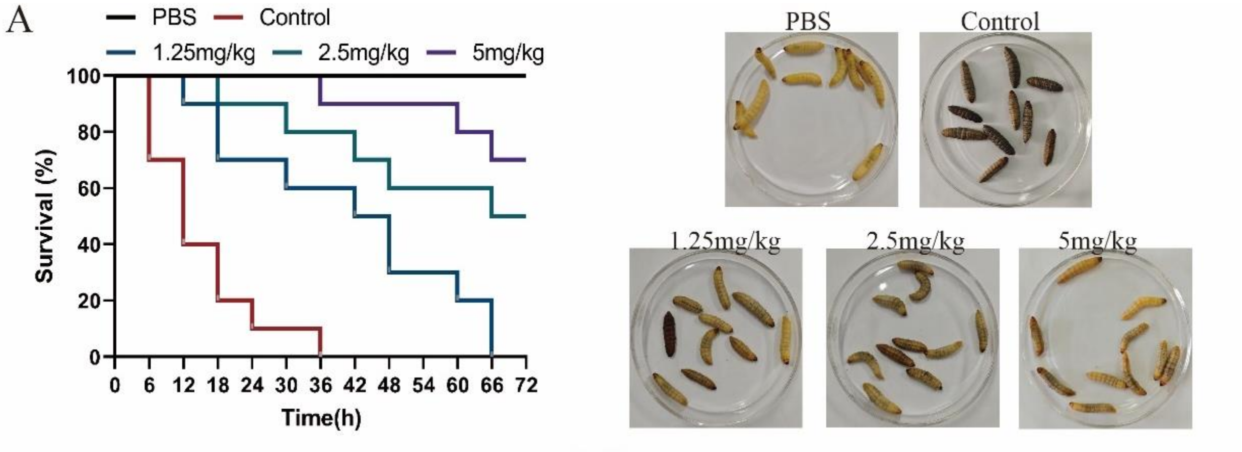

Strain : *ZY05719*

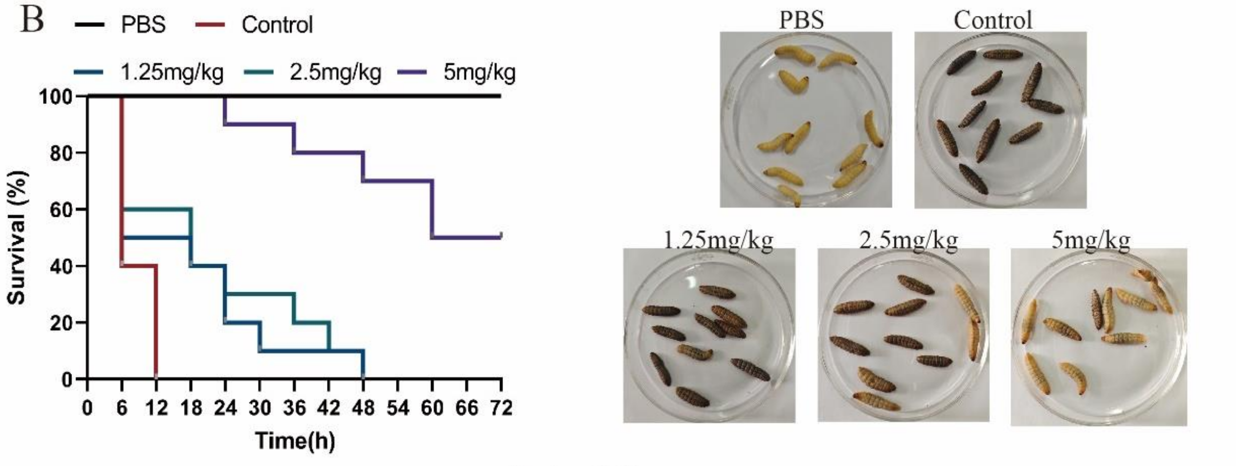

Strain : *P1/7*

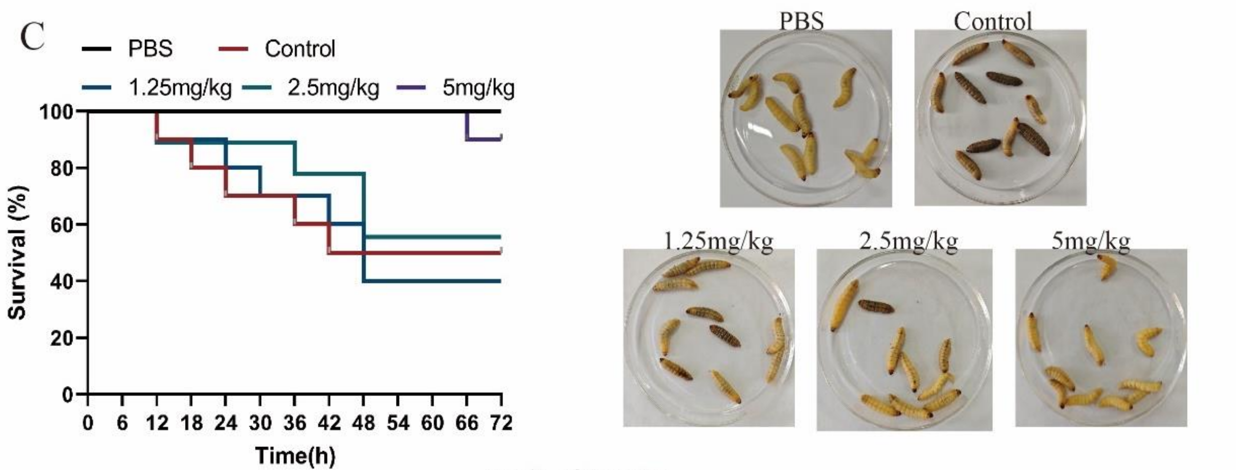

Strain : *SLYFP25*

Fig. S1: Therapeutic effects of SKQ1 across various *S. suis* infection models. A: Human isolate *(ZY05719)*. B: Highly virulent strain (*P1/7*). C: Multidrug-resistant strain (*SLYFP25*).

Table 1: Antibiotic susceptibility of SKQ1 against bacterial.

Strains	Characteristic	SKQ1(µg/mL)	
		MIC	MBC
S. aureus			
ATCC25923		2.5	2.5
SA 43300	MASR	2.5	2.5
E. faecalis			
E.f SC-8		5	10
E.f SC-9		5	5
S. agalactiae			
S. a SC-12		0.625	1.25
E. coli			
0157:H7	Human infection	80	80
K. pneumoniae			
KP SC-6		160	-
KP SC-7		160	-
B. bronchiseptica			
B.b D55		80	-
B.b Y221		40	-
Salmonella			
SM LY2031		160	-
SAT52		160	-
P. aeruginosa			
PA01		> 160	-
S. pneumoniae			
Spn4173		80	-

Sub-inhibitory concentrations of SKQ1 inhibit the biofilm formation of *S. suis:* Bacterial biofilms consist of microbial communities encased within a self-generated matrix of extracellular polymeric substances (Flemming *et al.*, 2016). Biofilms impede the action of bactericidal antibiotics and immune substances, shield bacteria from adverse conditions (e.g., immune responses), and enhance bacterial survival (Yin *et al.*, 2019; Yuan *et al.*, 2024). To further explore the antibacterial potential of SKQ1, we evaluated its effect on the biofilm-forming ability of *S. suis*. Sub-inhibitory concentrations of SKQ1 markedly inhibited biofilm formation by HA9801 (Fig. 3A). We broadened the scope of strains to validate SKQ1's inhibitory effect on biofilm formation. The results demonstrated that SKQ1 inhibited the biofilm-forming ability of multiple *S. suis* strains (Fig. 3B, 3C, 3D). To confirm this finding, we used scanning electron microscopy (SEM) to observe biofilm formation under SKQ1 treatment. These observations aligned with the crystal violet semi-quantitative assay results, demonstrating that sub-inhibitory concentrations of SKQ1 substantially impaired the biofilm-forming capacity of HA9801 (Fig. 3E). Given that extracellular polysaccharide (EPS) constitutes the primary component of biofilms (Flemming *et al.*, 2016)， we quantified EPS levels in *S. suis* following SKQ1 treatment. As expected, SKQ1 lowered EPS levels in a concentration-dependent manner (Fig. 3F). However, SKQ1 failed to eradicate mature biofilms (Fig. 3G). Bacteria within biofilms are highly resistant to various antibiotics, making infection treatment extremely challenging. Subsequently, we tested the bactericidal effect of SKQ1 on bacteria within biofilms. The results revealed that bactericidal concentrations of SKQ1 exhibited bactericidal activity against *S. suis* embedded within biofilms (Fig. 3H).

Sub-inhibitory concentrations of SKQ1 inhibit the virulence of *S. suis:* To further explore the antibacterial potential of SKQ1, we evaluated the effect of SKQ1 on the virulence of *S. suis* using the *Galleria mellonella* model. As shown in Fig. 4A, the entire control group of larvae succumbed within 18 hours. Treatment with 1/2 MIC of SKQ1 improved larval survival rates by 50% within 72 hours, while 1/4 and 1/8 MIC of SKQ1 increased survival rates by 10% during the same period. Similar inhibitory effects of SKQ1 on the virulence were observed in other *S. suis* strains (Fig. S3). Given SKQ1's known inhibitory effects on EPS production, we hypothesized that it might reduce the production of capsular polysaccharides (CPS) in *S. suis*, which are key virulence factors involved in immune evasion (Gao *et al.*, 2024a, 2024c). Quantitative measurements confirmed our hypothesis, showing that sub-inhibitory concentrations of SKQ1 significantly lowered CPS production in *S. suis* (Fig. 4B). Transmission electron microscopy further supported this finding, revealing that SKQ1 reduced CPS production in a dose-dependent manner (Fig. 4D). We next examined how SKQ1 affected the immune evasion capabilities of *S. suis*. The results indicated that SKQ1 reduced *S. suis*' capacity to evade phagocytosis by RAW264.7 macrophages (Fig. 4C). These findings suggest that the altered immune evasion ability associated with CPS production may be a key mechanism by which sub-inhibitory concentrations of SKQ1 influence the virulence of *S. suis*.

Untargeted metabolomics reveals that sub-inhibitory concentrations of SKQ1 disrupt methionine metabolism in *S. suis:* To investigate the underlying reasons for the reduced biofilm formation, virulence, EPS, and CPS production in *S. suis* grown under sub-inhibitory concentrations of SKQ1, untargeted metabolomics was performed to investigate metabolic disruptions induced by SKQ1 treatment. he PCA score plot revealed distinct clustering patterns and good reproducibility within each group (Fig. 5A), with a clear separation between the SKQ1-treated group and the control group, emphasizing the impact of SKQ1 on the metabolism of *S. suis*. Similarly, the heatmap revealed notable global metabolic differences between the SKQ1-treated and control groups (Fig. 5C). A total of 893 metabolites were detected and analyzed for metabolic changes. Using a significance threshold of $P < 0.01$, 176 metabolites were significantly downregulated, 83 were significantly upregulated, and 633 remained unchanged in the SKQ1-treated group (Fig. 5B). The differential metabolites were primarily enriched in pathways related to methionine metabolism, glycine and serine metabolism, glutamate metabolism, and purine metabolism (Figs. 5D and 5E). Notably, the overview of pathway enrichment for differentially detected metabolites revealed that the methionine metabolism pathway was the most significantly affected in *S. suis* following SKQ1 treatment (Fig. 5E). The primary methionine metabolism pathway in *S. suis*, including the AI-2 QS system, is depicted in Fig. 5F.

The AI-2 QS is a widely conserved intercellular communication mechanism in both Gram-positive and Gram-negative bacteria. The AI-2 signaling molecule is regulated by LuxS (S-ribosylhomocysteine lyase), a key enzyme within the methionine metabolism pathway (Fig. 5F). Numerous studies have demonstrated that the AI-2 QS system plays a central role in the life activities of *S. suis*, regulating various behaviors such as biofilm formation and virulence (Gao *et al.*, 2024a, 2024b). Based on the metabolomics results, we hypothesize that SKQ1 disrupts methionine metabolism, potentially altering the AI-2 QS system and its downstream regulatory processes, including biofilm formation and virulence.

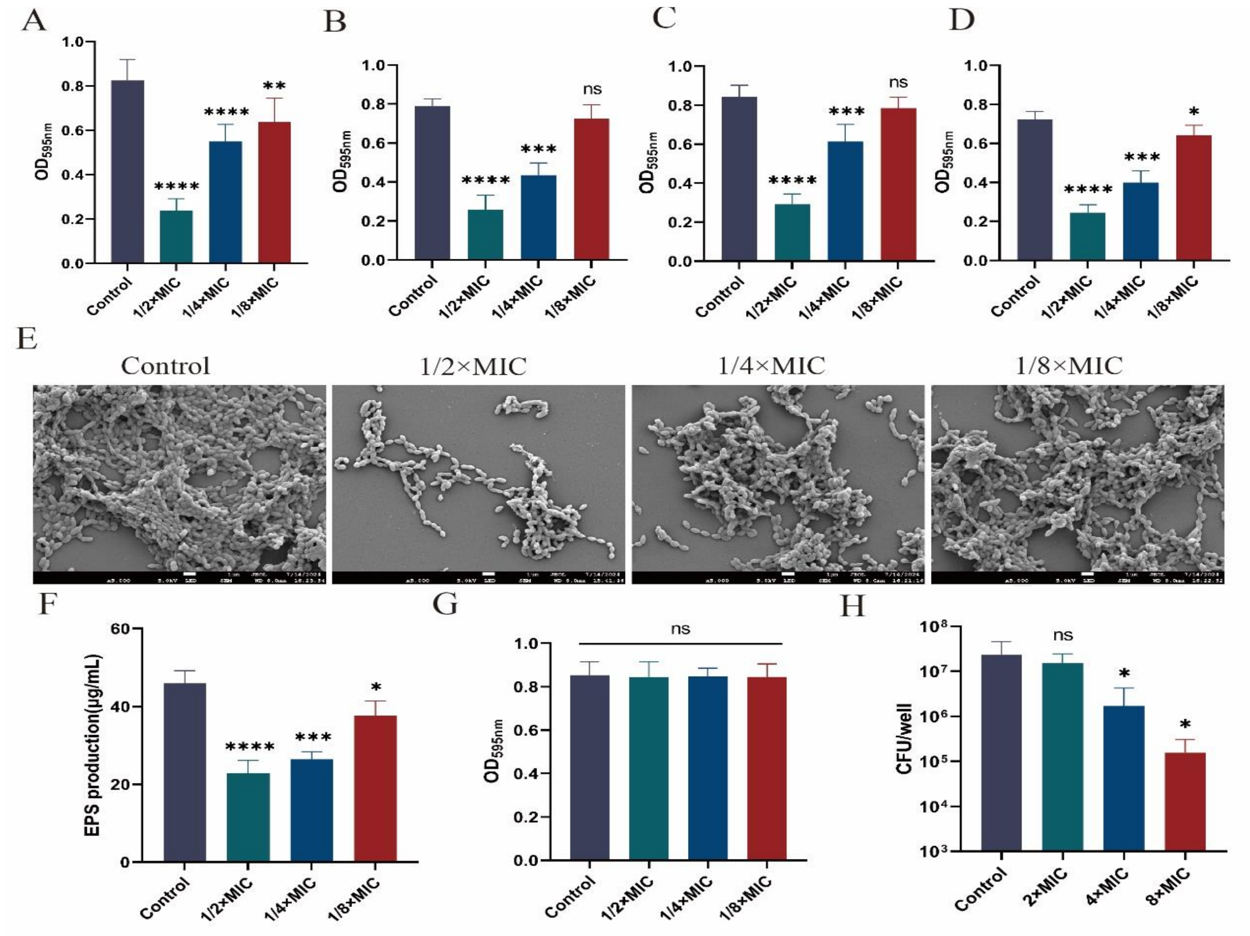

Fig. 3: Sub-inhibitory concentrations of SKQ1 inhibit the biofilm formation of *S. suis*. A-D: Effects of SKQ1 on biofilm formation across multiple *S. suis* strains. E: SEM images showing the biofilms of *S. suis* HA9801 after treatment with SKQ1. F: Quantification of EPS production by *S. suis* HA9801 following SKQ1 treatment. G: Effects of SKQ1 on the disruption of mature *S. suis* biofilms. H: Bactericidal activity of SKQ1 against *S. suis* within biofilms.

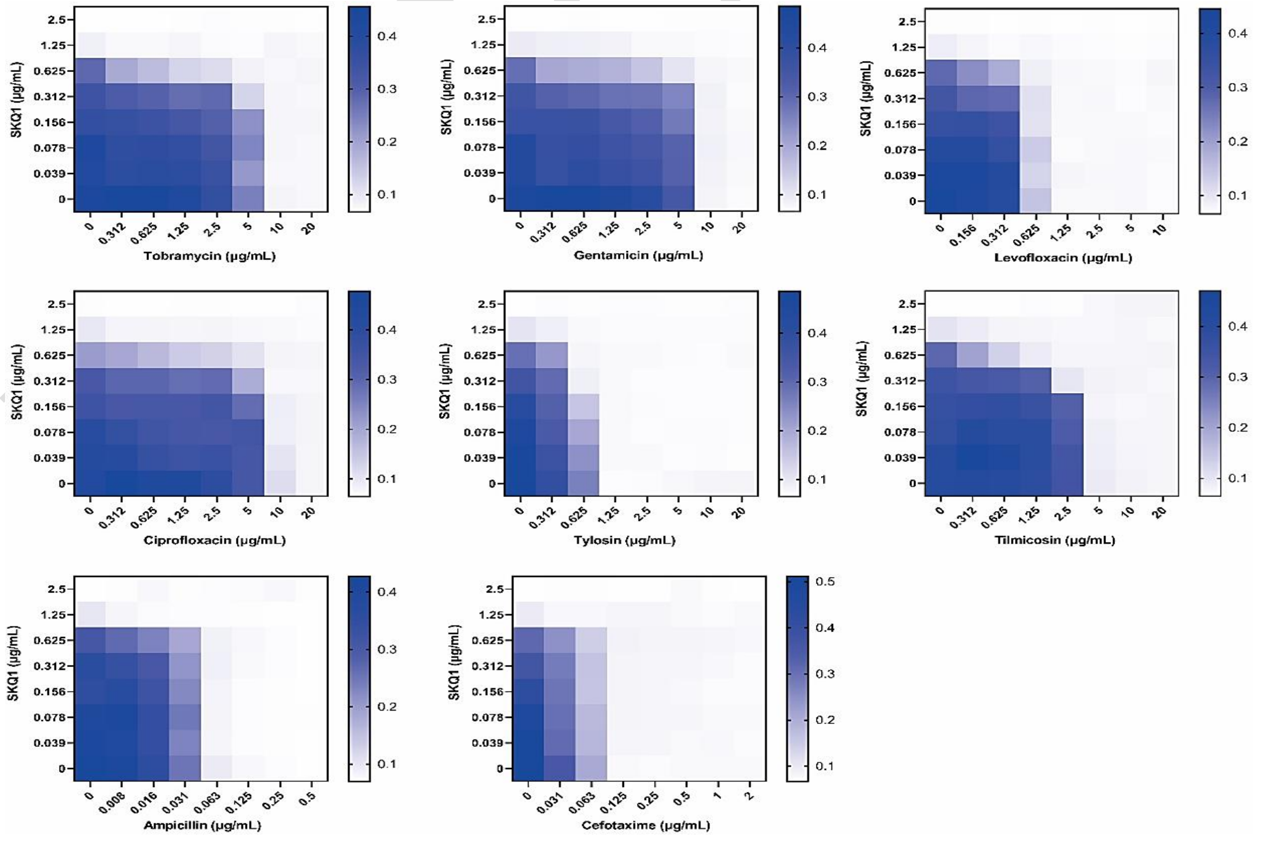

Fig. S3: Combinatory effects of SKQ1 with commonly used antibiotics.

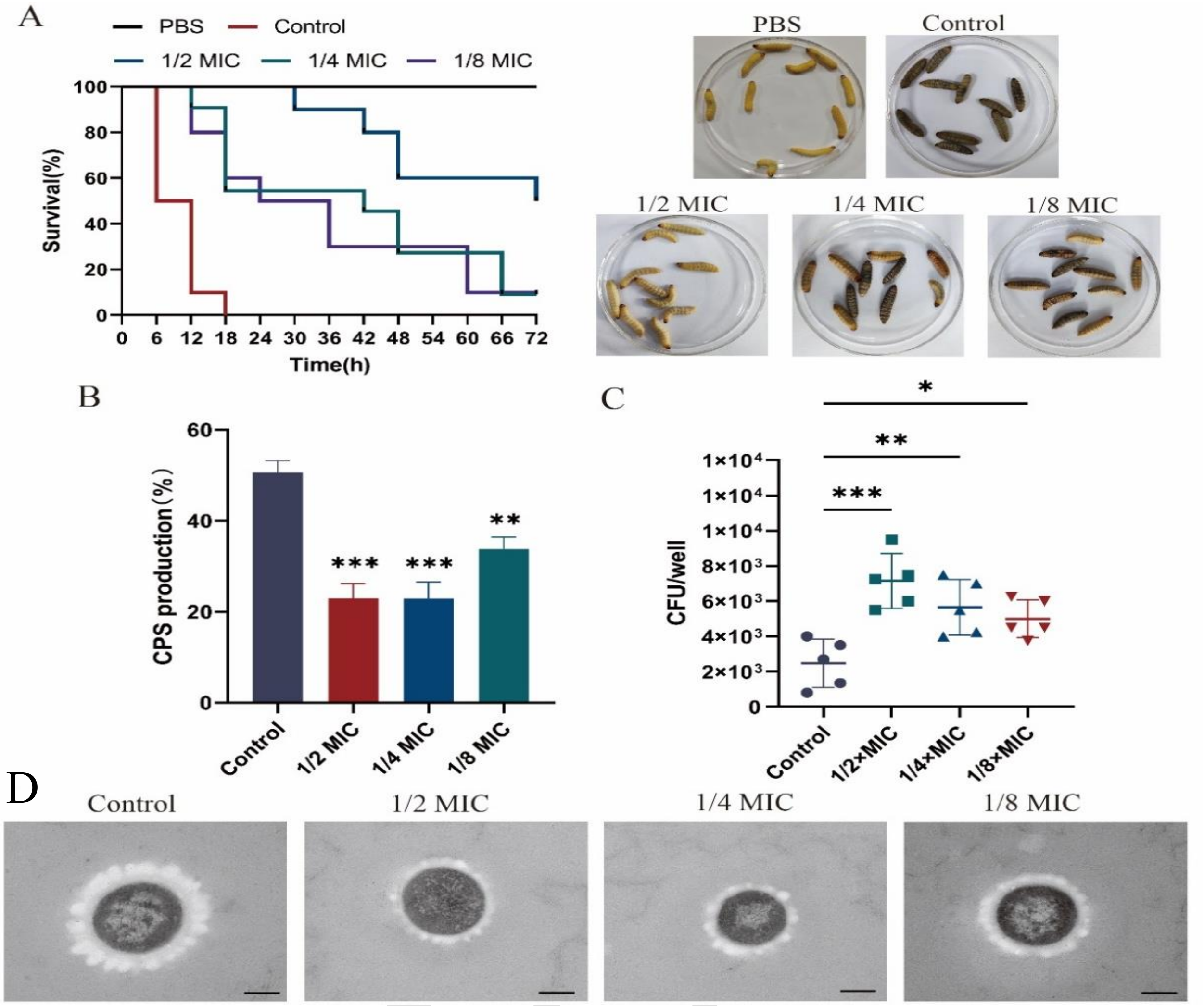

Fig. 4: Sub-inhibitory concentrations of SKQ1 inhibit CPS -associated virulence of *S. suis*. A: Lethality of *S. suis* to *Galleria mellonella* larvae following treatment with SKQ1. B: Impact of sub-inhibitory concentrations of SKQ1 on CPS production in *S. suis*. C: Effect of sub-inhibitory concentrations of SKQ1 on the anti-phagocytic ability of *S. suis*. D: TEM images showing changes in *S. suis* morphology and CPS layers after treatment with SKQ1.

SKQ1 inhibits the production of AI-2 QS signaling molecules, thereby regulating biofilm formation and virulence: To validate our hypothesis, we measured the AI-2 signaling molecule levels in *S. suis* after SKQ1 treatment. However, it was first necessary to rule out the possibility that the decrease in AI-2 production was due to SKQ1's inhibitory effect on bacterial growth. Therefore, we assessed the growth curves of *S. suis* in the presence of SKQ1. The results showed that SKQ1 at 1/2 and 1/4 MIC concentrations inhibited the growth of *S. suis*, while 1/8 MIC had no significant effect on bacterial growth (Fig. 6A). Thus, we selected the 1/8 MIC concentration for subsequent experiments. Using previously established methods, we measured AI-2 signaling molecule levels in *S. suis* with and without SKQ1 treatment. Consistent with our hypothesis, SKQ1 inhibited the production of AI-2 signaling molecules (Fig. 6B). To validate that SKQ1 affects biofilm formation and virulence through interference with the AI-2 QS system, we conducted experiments using a LuxS deletion strain (Δ*LuxS*) and exogenous supplementation of AI-2. As shown in the *Galleria mellonella* infection model (Fig. 6C), the virulence of Δ*LuxS* was significantly reduced compared to the wild-type strain. Exogenous AI-2 supplementation restored Δ*LuxS* virulence nearly to the wild-type level. In *S. suis* grown in 1/8 MIC SKQ1-treated media, larval mortality was significantly reduced. However, when exogenous AI-2 was added, virulence significantly increased but did not fully recover to WT level (Fig. 6C). This incomplete recovery may result from SKQ1's broad effects on multiple metabolic pathways in *S. suis* (Fig. 5E), causing partial virulence attenuation. Biofilm formation results were consistent with the virulence findings. Biofilm formation was significantly reduced in the Δ*luxS* mutant compared to the WT, which was partially restored with exogenous AI-2 supplementation (Fig. 6D). Similarly, SKQ1 at 1/8 MIC inhibited biofilm formation, but this inhibitory effect was partially counteracted by exogenous AI-2 supplementation (Fig. 6D). These results demonstrate that SKQ1 primarily interferes with the AI-2 QS system, reducing AI-2 production, thereby affecting *S. suis* biofilm formation and virulence.

Cytotoxicity of SKQ1: The cytotoxicity of SKQ1 was evaluated in vitro using the CCK-8 assay and a hemolysis test on porcine red blood cells. Results indicated that SKQ1 exhibited inhibitory effects on the viability of various mammalian cell lines, including PK-15, RAW264.7, Hep-2, and Marc-145. However, the half-maximal inhibitory concentration (IC50) values for all tested cell lines were significantly higher than the effective bactericidal concentration (4×MIC, 5 μg/mL) (Fig. 7A). Furthermore, SKQ1 displayed hemolytic activity on porcine red blood cells at concentrations of 32 μg/mL, whereas no hemolysis was observed at concentrations of 16 μg/mL or lower (Fig. 7B). Additional analysis focused on RAW264.7 macrophages and Hep-2 human cells, assessing Cell viabilities using Calcein-AM and PI staining. The results revealed that SKQ1, at concentrations of 8×MIC or lower, did not induce significant cell death in Hep-2 cells. However, treatment with 8×MIC SKQ1 increased the number of dead RAW264.7 cells (Fig. 7C). These findings suggest that while SKQ1 exhibits certain cytotoxic effects, it remains non-cytotoxic at effective antimicrobial concentrations, providing a promising therapeutic window.

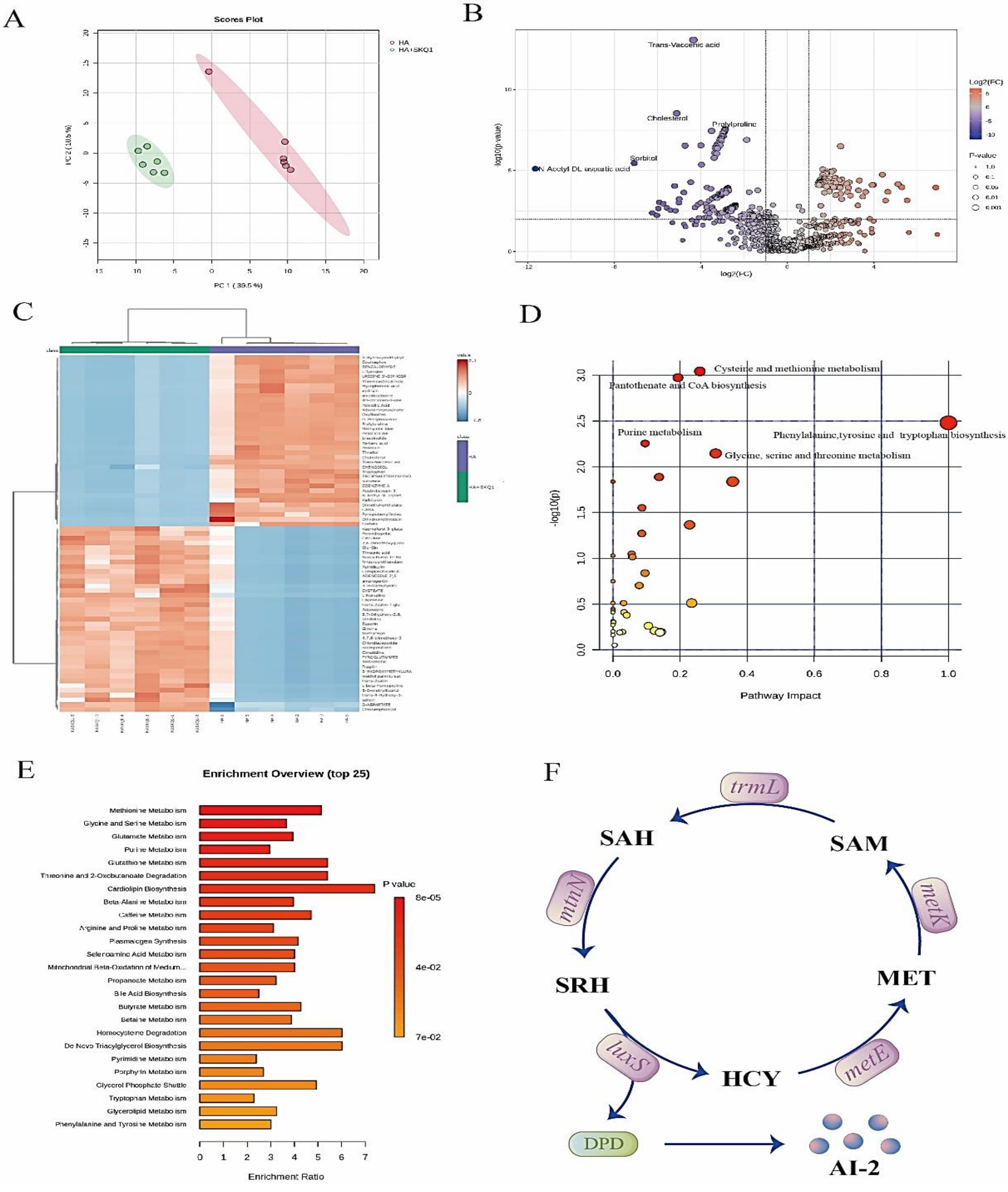

Fig. 5: Untargeted metabolomics analysis of the effects of SKQ1 on *S. suis*. A: PCA score plot of HA9801 and HA9801 + SKQ1 groups. B: Volcano plot of differentially detected metabolites. C: Heatmap showing metabolite profile differences between SKQ1-treated and control groups. D: Detailed metabolic pathways enriched with differentially detected metabolites. E: Overview of pathway enrichment for differentially detected metabolites. F: Primary methionine metabolism pathway.

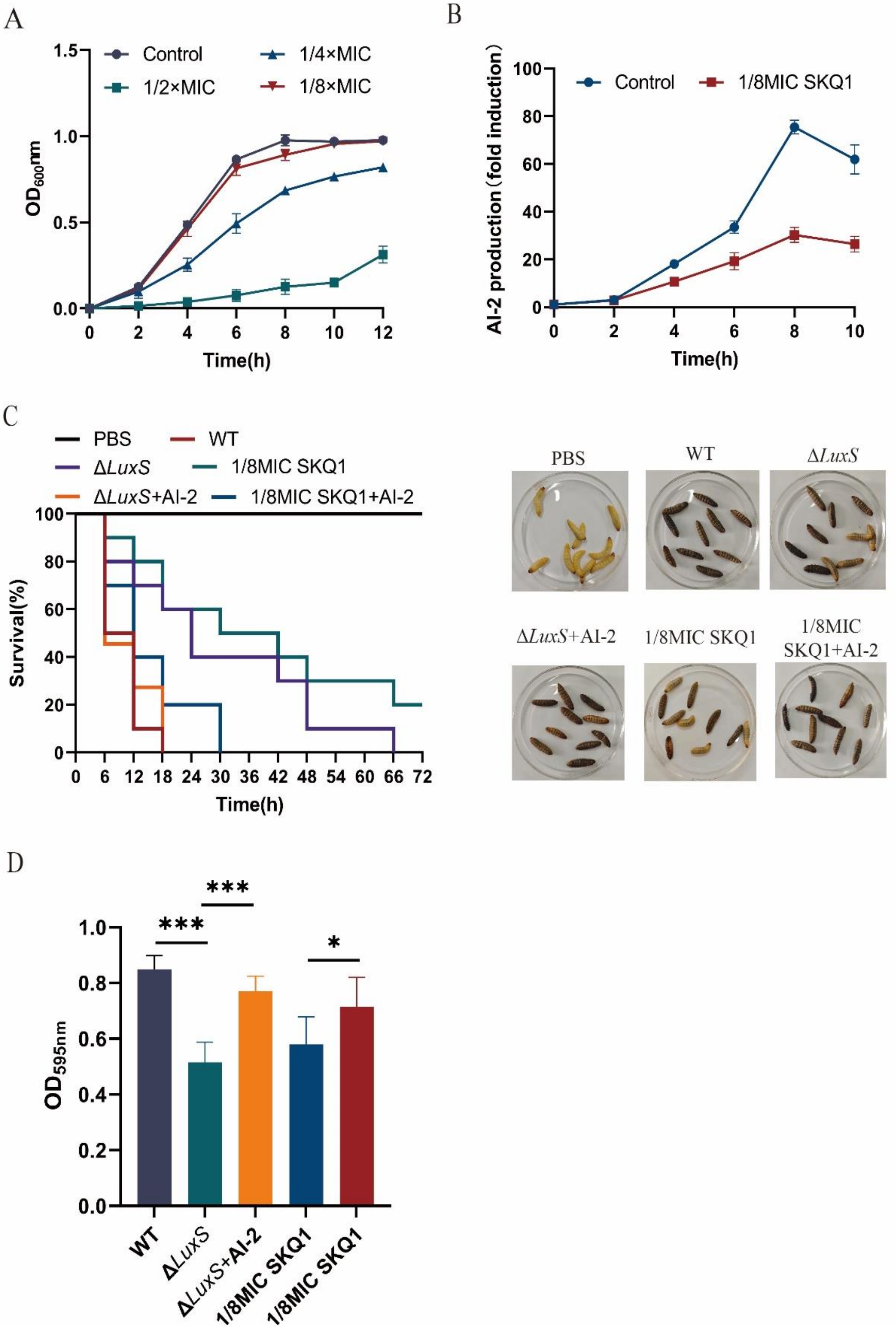

Fig. 6: SKQ1 inhibits the production of AI-2 QS signaling molecules, thereby regulating biofilm formation and virulence. A: Growth curves of *S. suis* treated with SKQ1. B: AI-2 signaling molecule production in *S. suis* after treatment with SKQ1. C: Lethality of Δ*LuxS* and WT strains treated with 1/8 MIC SKQ1 in the *Galleria mellonella* infection model, with or without exogenous AI-2 supplementation. D: Biofilm formation abilities of Δ*LuxS* and WT strains treated with 1/8 MIC SKQ1, with or without exogenous AI-2 supplementation.

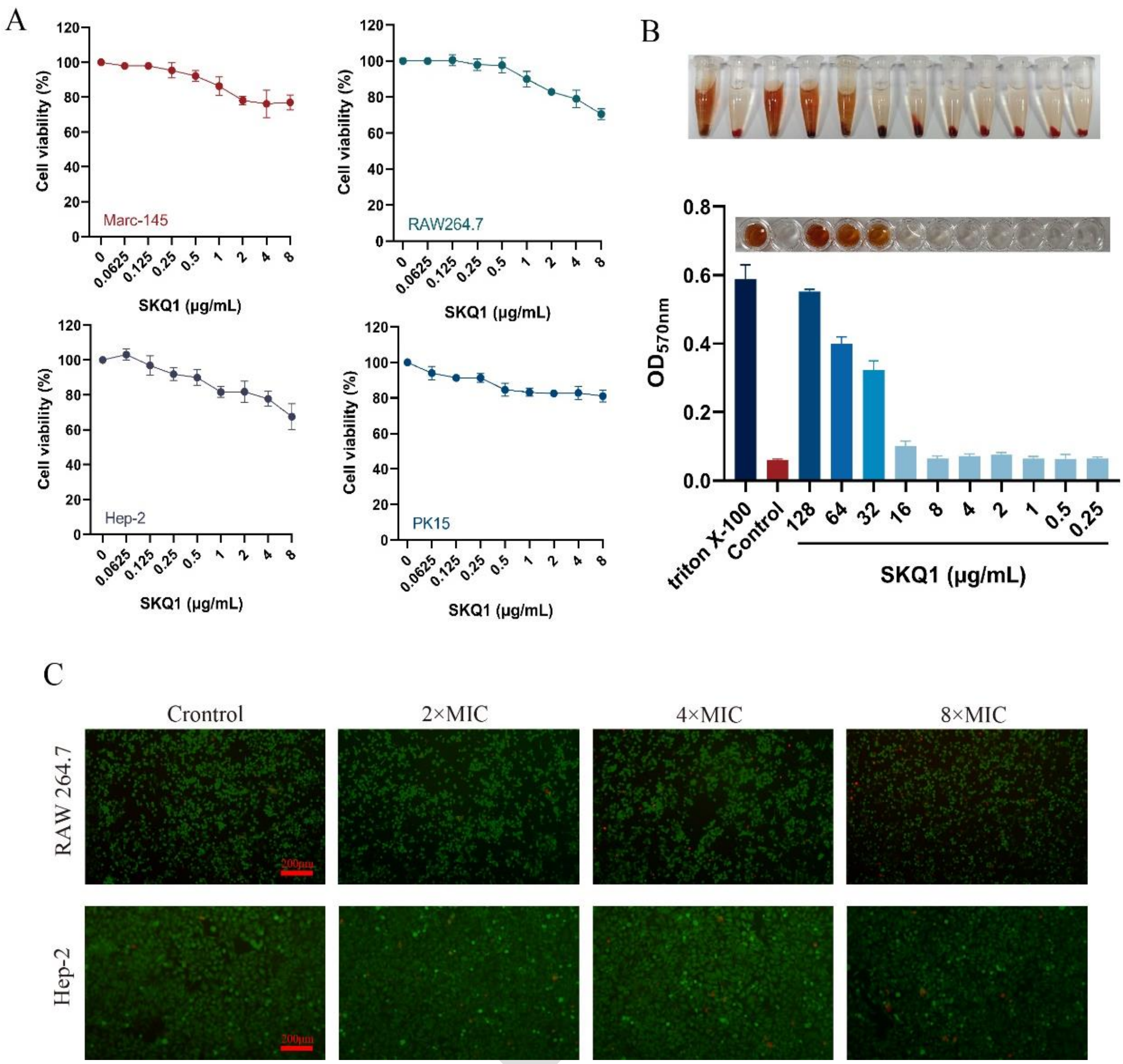

Fig. 7: Cytotoxicity of SKQ1. A: Inhibitory effects of SKQ1 on the viability of mammalian cell lines, including PK-15, RAW264.7, Hep-2, and Marc-145, determined by the CCK-8 assay. B: Hemolytic activity of SKQ1 on porcine red blood cells at various concentrations. C: Cytotoxic effects of SKQ1 on RAW264.7 macrophages and Hep-2 human cells, assessed using Calcein-AM and PI staining.

The combined effects of SKQ1 and commonly used antibiotics: Antibiotic adjuvant strategies have gained increasing attention due to their potential to reduce both time and economic costs compared to the development of new antibiotics. Given the unique bactericidal mechanism of SKQ1, we sought to evaluate its combinatory effects with other antibiotics that possess distinct mechanisms of action. We selected four antibiotic classes, each represented by two drugs: tobramycin and gentamicin (aminoglycosides); levofloxacin and ciprofloxacin (fluoroquinolones); tylosin and tilmicosin (macrolides); and ampicillin and cefotaxime (β-lactams). The checkerboard assay was employed to assess their combinatory effects with SKQ1 (Fig. S3). No synergistic effects were observed (fractional inhibitory concentration index [FICI] > 0.5); however, SKQ1 exhibited additive effects with the macrolides tylosin and tilmicosin (0.5<FICI<1), suggesting its potential to reduce the required dosage of these antibiotics (Fig. S3; Table S1).

Table S1: Antimicrobial effects of SKQ1 in combination with different classes of antibiotics against *S. suis*.

Antibiotic	MIC(μg/mL)	MIC with SKQ1(μg/mL)[a]	FICI[b]
Tobramycin	10	5	1
Gentamicin	10	5	1
Levofloxacin	0.625	0.625	1.25
Ciprofloxacin	10	5	1
Tylosin	5	1.25	0.75
Tilmicosin	1.25	0.625	0.75
Ampicillin	0.0625	0.0625	2
Cefotaxime	0.125	.0.125	2

[a]MIC in the presence of 0.625μg/mL of SKQ1. [b]Effects are defined as follows: synergy, FICI ≤ 0.5; additive, 0.5 <FICI < 1; indifferent, 1 ≤ FICI <4.

DISCUSSION

Antibiotic resistance is a major global health threat, accounting for approximately 9% of deaths worldwide (Bmbs, 2025). The excessive and improper use of antibiotics in agriculture and animal husbandry has accelerated the evolution of resistance in zoonotic pathogens, exacerbating the risk of infections (Bmbs, 2025;

Uruén *et al.*, 2022). Among these pathogens, *S. suis* is an emerging zoonotic bacterium that causes meningitis, toxic shock syndrome, and septicemia, with a mortality rate of approximately 12.8% (Huong *et al.*, 2014; Tang *et al.*, 2006). Alarmingly, the multidrug resistance (MDR) rate of *S. suis* has been rising rapidly in recent years, underscoring the urgent need for new antimicrobial strategies. However, the development of novel antibiotics faces significant challenges. Repurposing FDA-approved drugs with established safety profiles offers a time- and cost-efficient alternative. In this study, we identified SKQ1, a drug initially approved for treating dry eye syndrome, and evaluated its antibacterial activity against *S. suis*. SKQ1 exhibited strong inhibitory and bactericidal activities against multiple *S. suis* strains, including human isolates, hypervirulent strains, and MDR strains (Fig. 1C). In addition, SKQ1 showed pronounced antibacterial efficacy against Gram-positive species, including *Staphylococcus aureus* and *Streptococcus agalactiae*, while its activity against Gram-negative bacteria, such as *Salmonella* and *E. coli*, was comparatively limited (Table 1). This suggests that SKQ1 has a specific bactericidal effect on Gram-positive bacteria, likely due to its ability to penetrate the relatively simple and porous peptidoglycan layer of Gram-positive cell walls. In contrast, the outer membrane of Gram-negative bacteria, which contains lipopolysaccharides, acts as a barrier that limits the entry of many small molecules. Given that SKQ1 carries a positive charge, we hypothesized that it interacts with bacterial membranes via electrostatic forces, disrupting the cytoplasmic membrane and ultimately causing bacterial death. Scanning electron microscopy confirmed this hypothesis, showing that SKQ1 disrupted *S. suis* cell membranes in a dose-dependent manner, with higher concentration destroying bacterial morphology (Fig. 2D). Membrane permeability and nucleic acid leakage assays further supported this bactericidal mechanism (Fig. 2E, F). These findings align with previous studies on *S. aureus* (Wu *et al.*, 2024). However, SKQ1 appears to have multiple mechanisms of action. For instance, research by Dong *et al* 2023. demonstrated that SKQ1 kills *Mycobacterium tuberculosis* by targeting ribosomes and disrupting protein synthesis (Dong *et al.*, 2023) , while Nazarov *et al* 2023. showed that SKQ1 reduces membrane potential, impairing bacterial bioenergetics (Nazarov *et al.*, 2023a).

Antibiotic treatment failures often arise not only from resistance mutations but also from other mechanisms, such as persister formation (Gollan *et al.*, 2019) or bacterial evasion of antibiotics by residing within host cells (Liu *et al.*, 2020b). Notably, SKQ1 displayed potent bactericidal activity against both *S. suis* persisters and intracellular *S. suis* (Fig. 2B, C). Persisters are characterized by a dormant state with low metabolic activity, making them less susceptible to antibiotics targeting biosynthetic processes, such as DNA or protein synthesis (Conlon *et al.*, 2016; Ea *et al.*, 2019; Stokes *et al.*, 2019). SKQ1, however, disrupts the bacterial cytoplasmic membrane, a mechanism independent of metabolic state, which may explain its efficacy against persisters. Additionally, SKQ1's ability to penetrate mammalian cell membranes enables it to kill intracellular *S. suis*. These findings highlight SKQ1 as a promising candidate for treating *S. suis* infections, including those involving persisters or intracellular bacteria. It should be noted that although the immune system of *G. mellonella* shares considerable similarity with that of mammals (Tsai, Loh, and Proft, 2016), direct evidence regarding the pharmacokinetics and therapeutic efficacy of SKQ1 in mammals is still lacking. Future studies using mammalian models such as mice or piglets are needed to further validate its in vivo potential.

It is well-established that the AI-2 QS system plays a pivotal role in regulating the biological activities of *S. suis*, including monosaccharide metabolism, biofilm formation, antibiotic resistance, and virulence (Gao *et al.*, 2024a, 2024b; Liu *et al.*, 2020a; Wang *et al.*, 2018, 2019). In this study, we found that subinhibitory concentrations of SKQ1 significantly suppressed the biofilm formation capacity and capsule polysaccharide-associated virulence of *S. suis* (Fig. 3A, 4A). This inhibitory effect was observed across multiple *S. suis* strains (Fig. S2). Untargeted metabolomics revealed that these effects of SKQ1 may be mediated through interference with methionine metabolism, which subsequently affects AI-2 production. This mechanism is similar to that of the widely studied QS inhibitor 5-FU (Sedlmayer *et al.*, 2021; Zuo *et al.*, 2024). Further experiments measuring AI-2 production after SKQ1 treatment supported the predictions from metabolomics data. At concentrations that did not affect *S. suis* growth, SKQ1 significantly inhibited AI-2 production (Fig. 6B). Advances in the in vitro synthesis of 4,5-dihydroxy-2,3-pentanedione (DPD), the precursor of AI-2, have enabled the production of bioactive synthetic AI-2. The ability of synthetic AI-2 to rescue the phenotypes of Δ*LuxS* mutants further validates the regulatory role of AI-2 in *S. suis*. In this study, exogenous supplementation with synthetic AI-2 partially reversed the inhibitory effects of SKQ1 on biofilm formation and virulence in S. suis, further confirming its suppression of AI-2 production (Fig. 6C, 6D). Interestingly, SKQ1 has also been reported to inhibit *S. aureus* biofilm formation and hemolysis by downregulating the expression of genes related to the agr QS system (Wu *et al.*, 2024). These results suggest that SKQ1 may target multiple QS systems. The dual antibacterial and anti-QS activities of SKQ1 against both *S. aureus* and *S. suis* highlight its potential for treating mixed infections. However, further studies are necessary to explore this potential and to elucidate the precise mechanisms underlying its QS inhibitory effects.

Although SKQ1 exhibited remarkable antibacterial and QS inhibitory activities, it is important to note that SKQ1 also demonstrated a certain degree of cytotoxicity (Fig. 7). SKQ1 and its structurally related derivatives are generally considered cytotoxic, as studies have shown that treatment with SKQ1 at concentrations above 1 μM reduces cellular viability and metabolic activity (Fernandes *et al.*, 2021). However, the extent of SKQ1's cytotoxicity may have been overestimated. Recent studies revealed that at concentrations below 5 μM, SKQ1 primarily inhibits cellular metabolism, whereas the cytotoxicity observed at concentrations above 5 μM may be attributed to its effects on cellular adhesion capacity (Nazarov *et al.*, 2023b). A more detailed toxicological analysis can be found in Nazarov *et al.*, 2023b. This aligns with our findings: compared to Hep-2 cells, SKQ1 exhibited higher toxicity toward RAW264.7 cells, potentially due to the lower

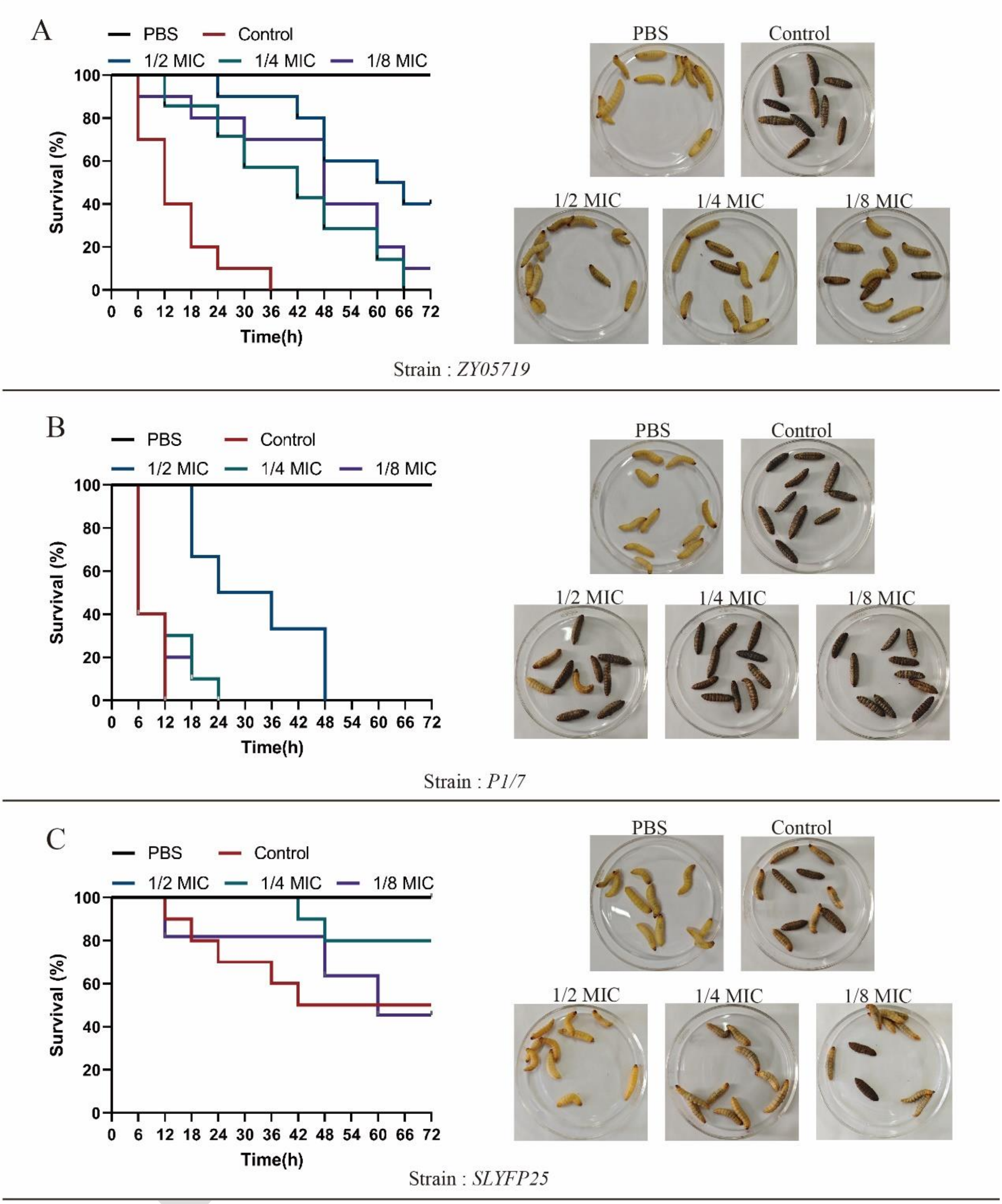

Fig. S2: Inhibitory effects of SKQ1 on the virulence of *S. suis* strains with different characteristics. A: Effect of SKQ1 on the virulence of *ZY05719*. B: Effect of SKQ1 on the virulence of *P1/7*. C: Effect of SKQ1 on the virulence of *SLYFP25*.

adhesion capacity of RAW264.7 cells (Fig. 7C). Importantly, in vivo, a reduction in cellular adhesion capacity may not necessarily result in significant tissue damage. Supporting this, SKQ1 has been shown to promote health and extend the lifespan of mice at concentrations exhibiting antimicrobial effects (Shabalina *et al.*, 2017). In our study, while SKQ1 was found to inhibit cellular activity, it did not exhibit significant cytotoxic effects on mammalian cells within its effective bactericidal concentration range (Fig. 7).

Conclusions: In summary, SKQ1 exerts its antibacterial effects against *S. suis* through dual mechanisms. At high concentrations, SKQ1 disrupts the bacterial cytoplasmic membrane, leading to cell death. At sub-inhibitory concentrations, SKQ1 interferes with methionine metabolism, thereby suppressing the AI-2 QS system and inhibiting *S. suis* biofilm formation and virulence. These findings provide valuable insights into the antibacterial mechanisms of SKQ1 and suggest its potential as a therapeutic agent for *S. suis* infections or as a basis for developing novel QS inhibitors.

Funding: This research was financially supported by the National Natural Science Foundation of China (32573360, 32172852), Scientific and Technological Innovation Leaders in Central Plains (254200510022), Program for Innovative Research Team (in Science and Technology) in University of Henan Province (24IRTSTHN033) and Key Scientific Research Projects of Higher Education Institutions of Henan Province (24A230013).

Author contributions: SY Conceptualization, Formal analysis, Methodology, Writing – original draft, Writing – review and editing; ZY Methodology, Validation, Writing – original draft, Writing – review and editing; JW Formal analysis, Methodology, Writing –review and editing; SG Methodology, Writing – review and editing; YQ Methodology, Writing – review and editing; WJ Methodology, Writing – review and editing; BL Methodology, Writing – review and editing; YW Software, Visualization; SW Formal analysis, Writing – review and editing; YL Formal analysis, Writing – review and editing; YW Conceptualization, Project administration, Supervision, Writing – original draft, Writing – review and editing.

Competing interests: All authors declare they have no competing interests.

Data and materials availability: Data will be made available on request.

REFERENCES

Abisado RG, Benomar S, Klaus JR, *et al.*, 2018. Bacterial Quorum Sensing and Microbial Community Interactions. mBio 9:e02331-17.

Bmbs CSH, 2025. Antimicrobial resistance: a concise update. 6.

Conlon BP, Rowe SE, Gandt AB, *et al.*, 2016. Persister formation in *Staphylococcus aureus* is associated with ATP depletion. Nat Microbiol 1:16051.

Dong WQ, Wang GY, Bai YJ, *et al.*, 2023. Repurposing an Antioxidant to Kill *Mycobacterium tuberculosis* by Targeting the 50S Subunit of the Ribosome. Biomolecules 13:1793.

Ea Z, As N, S M, *et al.*, 2019. Stochastic Variation in Expression of the Tricarboxylic Acid Cycle Produces Persister Cells. mBio 10.

Fan Q, Zuo J, Wang H, *et al.*, 2022. Contribution of quorum sensing to virulence and antibiotic resistance in zoonotic bacteria. Biotechnol Adv 59:107965.

Fernandes C, Videira AJC, Veloso CD, *et al.*, 2021. Cytotoxicity and Mitochondrial Effects of Phenolic and Quinone-Based Mitochondria-Targeted and Untargeted Antioxidants on Human Neuronal and Hepatic Cell Lines: A Comparative Analysis. Biomolecules 11:1605.

Flemming H-C, Wingender J, Szewzyk U, *et al.*, 2016. Biofilms: an emergent form of bacterial life. Nat Rev Microbiol 14:563–575.

Gao S, Yuan S, Quan Y, *et al.*, 2025. Targeting AI-2 quorum sensing: harnessing natural products against *streptococcus suis* biofilm infection. Vet Res 56:26.

Gao SJ, Mao CL, Yuan S, *et al.*, 2024a. AI-2 quorum sensing-induced galactose metabolism activation in *Streptococcus suis* enhances capsular polysaccharide-associated virulence. Vet Res 55:80.

Gao SJ, Yuan S, Quan YY, *et al.*, 2024b. Effects of AI-2 quorum sensing related luxS gene on *Streptococcus suis* formatting monosaccharide metabolism-dependent biofilm. Arch Microbiol 206:407.

Gao SJ, Jin WJ, Quan YY, *et al.*, 2024c. Bacterial capsules: Occurrence, mechanism, and function. NPJ Biofilms Microbiomes 10:21.

Gollan B, Grabe G, Michaux C, *et al.*, 2019. Bacterial Persisters and Infection: Past, Present, and Progressing. Annu Rev Microbiol 73:359–385.

Han XG and Lu CP, 2009. In vitro biosynthesis of autoinducer 2 of *Steptococcus suis* Serotype 2 using recombinant LuxS and Pfs. Enzyme Microb Technol 44:40–45.

Hoa NT, Chieu TTB, Nghia HDT, *et al.*, 2011. The antimicrobial resistance patterns and associated determinants in *Streptococcus suis* isolated from humans in southern Vietnam, 1997-2008. BMC Infect Dis 11:6.

Huong VTL, Ha N, Huy NT, *et al.*, 2014. Epidemiology, clinical manifestations, and outcomes of *Streptococcus suis* infection in humans. Emerg Infect Dis 20:1105–1114.

Kennedy D, Cronin UP, Piterina AN, *et al.*, 2019. Heat and Chemical Treatments Affect the Viability, Morphology, and Physiology of *Staphylococcus aureus* and Its Subsequent Antibody Labeling for Flow Cytometric Analysis. Appl Environ Microbiol 85:e01006-19.

Li J, Fan Q, Zuo J, *et al.*, 2022. Paeoniflorin combined with norfloxacin ameliorates drug-resistant *streptococcus suis* infection. J Antimicrob Chemother 77:3275–3282.

Li Q, Feng HZ, Tian Q, *et al.*, 2024. Discovery of antibacterial diketones against gram-positive bacteria. Cell Chem Biol 31:1874-1884.e6.

Liu BB, Yi L, Li JP, *et al.*, 2020a. Autoinducer-2 influences tetracycline resistance in *Streptococcus suis* by regulating the tet(M) gene via transposon Tn916. Res Vet Sci 128:269–274.

Liu X, Liu F, Ding S, *et al.*, 2020b. Sublethal levels of antibiotics promote bacterial persistence in epithelial cells. Adv Sci Weinh Baden-Wurtt Ger 7:1900840.

Lun Z-R, Wang Q-P, Chen X-G, *et al.*, 2007. *Streptococcus suis*: an emerging zoonotic pathogen. Lancet Infect Dis 7:201–209.

Nazarov PA, Majorov KB, Apt AS, *et al.*, 2023a. Penetration of Triphenylphosphonium Derivatives through the Cell Envelope of Bacteria of *Mycobacteriales* Order. Pharm Basel Switz 16:688.

Nazarov PA, Khrulnova SA, Kessenikh AG, *et al.*, 2023b. Observation of Cytotoxicity of Phosphonium Derivatives Is Explained: Metabolism Inhibition and Adhesion Alteration. Antibiot Basel Switz 12:720.

Novikova YP, Gancharova OS, Eichler OV, *et al.*, 2014. Preventive and therapeutic effects of SkQ1-containing Visomitin eye drops against light-induced retinal degeneration. Biochem Biokhimiia 79:1101–1110.

Obradovic MR, Segura M, Segalés J, *et al.*, 2021. Review of the speculative role of co-infections in *Streptococcus suis*-associated diseases in pigs. Vet Res 52:49.

Pang ZQ, Lu Y, Zhou GY, *et al.*, 2024. MetaboAnalyst 6.0: towards a unified platform for metabolomics data processing, analysis and interpretation. Nucleic Acids Res 52:W398–W406.

Sedlmayer F, Woischnig A-K, Unterreiner V, *et al.*, 2021. 5-Fluorouracil blocks quorum-sensing of biofilm-embedded methicillin-resistant *Staphylococcus aureus* in mice. Nucleic Acids Res 49:e73.

Shabalina IG, Vyssokikh MY, Gibanova N, *et al.*, 2017. Improved health-span and lifespan in mtDNA mutator mice treated with the mitochondrially targeted antioxidant SkQ1. Aging 9:315–339.

Stokes JM, Lopatkin AJ, Lobritz MA, *et al.*, 2019. Bacterial Metabolism and Antibiotic Efficacy. Cell Metab 30:251–259.

Sun Y, Wu Y, Chang Y, *et al.*, 2025. Exploring the antibacterial and anti-biofilm properties of diacerein against methicillin-resistant *Staphylococcus aureus*. Front Microbiol 16:1545902.

Surette MG and Bassler BL, 1998. Quorum sensing in *Escherichia coli* and Salmonella typhimurium. Proc Natl Acad Sci U S A 95:7046–7050.

Tang J, Wang C, Feng Y, *et al.*, 2006. Streptococcal toxic shock syndrome caused by *streptococcus suis* serotype 2. PLoS Med 3:e151.

Tang ZY, Feng JZ, Challa M, *et al.*, 2024. Discovery of novel Thymol-TPP antibiotics that eradicate MRSA persisters. Eur J Med Chem 270:116381.

Tsai CJ-Y, Loh JMS and Proft T, 2016. Galleria mellonella infection models for the study of bacterial diseases and for antimicrobial drug testing. Virulence 7:214–229.

Uruén C, García C, Fraile L, *et al.*, 2022. How *Streptococcus suis* escapes antibiotic treatments. Vet Res 53:91.

Van Boeckel TP, Brower C, Gilbert M, *et al.*, 2015. Global trends in antimicrobial use in food animals. Proc Natl Acad Sci U S A 112:5649–5654.

Wang Y, Wang YX, Sun LY, *et al.*, 2018. The LuxS/AI-2 system of *Streptococcus suis*. Appl Microbiol Biotechnol 102:7231–7238.

Wang Y, Liu BB, Li JP, *et al.*, 2019. LuxS/AI-2 system is involved in fluoroquinolones susceptibility in *Streptococcus suis* through overexpression of efflux pump SatAB. Vet Microbiol 233:154–158.

Wei Y, Troger A, Spahiu V, *et al.*, 2019. The Role of SKQ1 (Visomitin) in Inflammation and Wound Healing of the Ocular Surface. Ophthalmol Ther 8:63–73.

Werinder A, Aspán A, Backhans A, *et al.*, 2020. *Streptococcus suis* in Swedish grower pigs: occurrence, serotypes, and antimicrobial susceptibility. Acta Vet Scand 62:36.

Willenborg J, Willms D, Bertram R, *et al.*, 2014. Characterization of multi-drug tolerant persister cells in *streptococcus suis*. BMC Microbiol 14:120.

Wu R, Wu Y, Wu P, *et al.*, 2024. Bactericidal and anti-quorum sensing activity of repurposing drug Visomitin against *Staphylococcus aureus*. Virulence 15:2415952.

Yin W, Y W, L L, *et al.*, 2019. Biofilms: The Microbial "Protective Clothing" in Extreme Environments. Int J Mol Sci 20.

Yuan S, Shen YM, Quan YY, *et al.*, 2024. Molecular mechanism and application of emerging technologies in study of bacterial persisters. BMC Microbiol 24:480.

Yuan S, Liu B, Quan Y, *et al.*, 2025. *Streptococcus suis* regulates central carbon fluxes in response to environment to balance drug resistance and virulence. Microbiol Res 296:128157.

Zhang M, Song H, Yang S, *et al.*, 2024. Deciphering the antibacterial mechanisms of 5-fluorouracil in *Escherichia coli* through biochemical and transcriptomic analyses. Antibiot Basel Switz 13:528.

Zuo J, Quan Y, Li J, *et al.*, 2024. Tackling antibiotic resistance: exploring 5-fluorouracil as a promising antimicrobial strategy for the treatment of *streptococcus suis* infection. Animals Open Access J MDPI 14:1286.